ARCHIVES OF METALLURGY AND MATERIALS
Volume 51 2006 Issue 2

K. ZIEWIEC* P. KURTYKA*

DETERMINATION OF THERMAL AND MECHANICAL PROPERTIES OF $Ni_{63}Cu_9Fe_8P_{20}$ AMORPHOUS ALLOY

BADANIE WŁAŚCIWOŚCI CIEPLNYCH I MECHANICZNYCH AMORFICZNEGO STOPU $Ni_{63}Cu_9Fe_8P_{20}$

Nickel-copper-iron-phosphorus $Ni_{63}Cu_9Fe_8P_{20}$ alloy was cast using melt spinning method. The ribbons in as cast state are characterized with use of TEM and X-ray diffraction. Then the ribbons were heated in DTA up to different temperatures and then characterized with use of X-ray diffraction to see the change of the microstructure after heating to elevated temperatures. The melt-spun ribbons in as-cast state were preliminarily compacted in a die and then compressed. The mechanical characteristics of the compacted ribbons at different temperatures were registered.

Keywords: melt spinning, metallic glass, glass forming ability, thermal stability, crystallization, mechanical properties

Stop niklu, miedzi, żelaza i fosforu o składzie $Ni_{63}Cu_9Fe_8P_{20}$ odlewano metodą „melt spinning". Otrzymane taśmy w stanie po odlewaniu były badane przy pomocy transmisyjnego mikroskopu elektronowego (TEM) oraz dyfraktometru rentgenowskiego. Następnie taśmy nagrzewano w różnicowym analizatorze termicznym (DTA) do różnych temperatur a następnie były one ponownie badane przy pomocy dyfraktometru rentgenowskiego. Po odlewaniu metodą „melt spinning" taśmy były wstępnie prasowane w matrycy w celu otrzymania pastylek a następnie poddawane próbie ściskania. Rejestrowano charakterystyki mechaniczne prasowanych taśm przy różnych temperaturach.

1. Introduction

Amorphous metallic alloys have been developed recently in many multi-component systems [1–3]. The metallic glasses have interesting properties, e.g. high elasticity limit and low coercivity. These characteristics, which can be hardly found in crystalline materials, are attractive for practical uses of structural and functional materials. The characteristics of metallic glasses are strongly temperature dependent. Amorphous metallic alloys often show significant plasticity in the supercooled liquid region. It is reported that it is due to a substantial drop of viscosity by several orders of magnitude [4, 5]. The feature can be potentially used in forming bulk shapes starting from the glassy alloys that are not necessarily the best glass formers [6, 7]. Recently, several glassy alloys with a wide supercooled liquid region and substantial glass forming ability were elaborated [8–14]. Due to the limited resources and high prices of such constituents as Pd, La, Nd and Zr, applications of metallic glasses with high glass forming ability are still very restricted. Therefore, more common use of good glass forming liquids lies probably behind the use of other precursors that possibly could improve glass forming ability or provide a large supercooled liquid region. On the other hand, analysis of available binary and ternary phase diagrams containing Ni, Cu, Fe and P indicates that especially in compositions where one of the constituents is P there are deep eutectics [15] and in Ni-Cu-Fe-P system good glass forming ability can be expected [12]. The Ni-Cu-Fe-P alloys present also supercooled liquid region [16].

The present study reports the behaviour of amorphous $Ni_{63}Cu_9Fe_8P_{20}$ melt spun alloy during the non-isothermal heating and compressing tests of pre-compacted ribbons performed at different temperatures. We compare the non-elastic behaviour of the ribbons and compressing tests of the pre-compacted samples with the DTA traces and the results of X-ray diffractions after heating to different temperatures.

2. Experimental

Nickel-copper-iron-phosphorus $Ni_{63}Cu_9Fe_8P_{20}$ alloy was cast using melt spinning with linear rate of 23 m/s (approximate cooling rate of 10^5 K/s). The ribbon in the

* FACULTY OF MATHEMATICS, PHYSICS AND TECHNICAL SCIENCES, PEDAGOGICAL UNIVERSITY, 30-084 KRAKÓW, PODCHORĄŻYCH 2 STR., POLAND

as-cast state was tested by TEM and X-ray diffraction to check whether it is amorphous. The melt-spun ribbons were then coiled and investigated by means of differential thermal analysis (DTA – STD 2960 TA Instruments) at the heating rate of 10 K/min. The heating cycles were stopped at different temperatures: 473K, 523K, 613K, 633K, 643K, 673K and 723K. The coiled samples were photographed and their external diameters after interrupted DTA cycle were measured. Then X-ray diffraction measurements of the coils were performed using Siemens D5005 (Bruker-AXS) diffractometer equipped with Cu lamp with 30mA and 40kV power supply. Phase identification was made using JCPDS database [17]. The radiation was monochromatized with graphite monochromator. In some measurements high purity silicon placed on the plate was used as an external standard to ensure the correct sample position during the operation. Then the as-cast melt-spun ribbon was preliminarily compacted in a die to form 10 mm diameter, 2 g samples with use of 5 kN load. After pre-pressing (Fig. 1a) the samples were compressed between plates (Fig. 1b) at different temperatures in INSTRON TT-DM (100 kN) testing machine. The time used for stabilization of the temperature was 30 min. After this period, the load – deformation characteristics were registered.

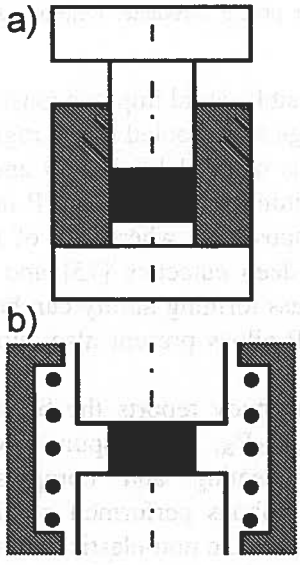

Fig. 1. The diagram showing: a) preliminary compaction of ribbons in a die; b) compressing the samples between plates in a furnace

3. Results and discussion

The TEM micrograph and electron diffraction pattern of the as-cast sample is presented on Fig. 2. The amorphous microstructure is uniform and does not show contrast variations which is confirmed by the electron diffraction pattern presenting broad diffusive rings.

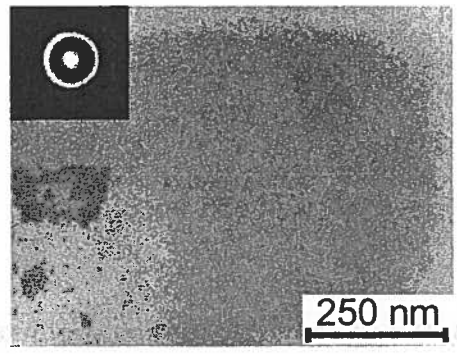

Fig. 2. TEM microstructure with electron diffraction patterns from the amorphous $Ni_{63}Cu_9Fe_8P_{20}$

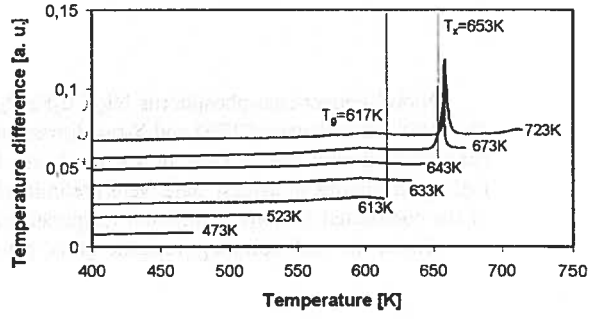

Fig. 3. DTA curves registered for coiled ribbon of the amorphous $Ni_{63}Cu_9Fe_8P_{20}$ alloy. The thermal cycles where stopped at different temperatures

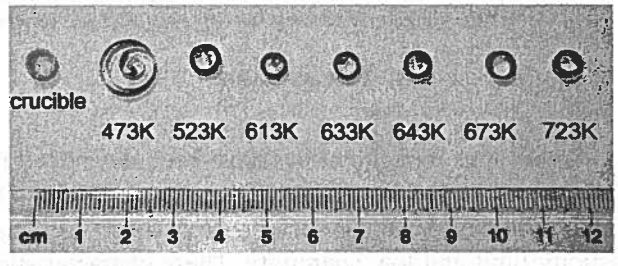

Fig. 4. The appearance of the coils from DTA cycles stopped at different temperatures

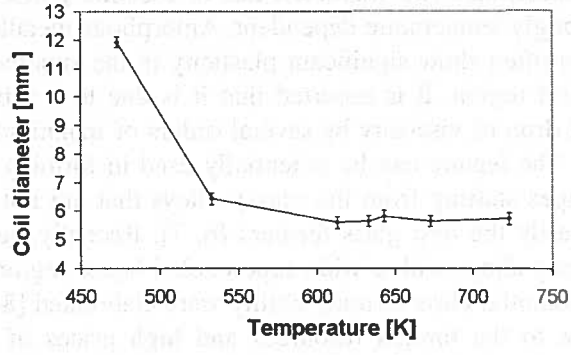

Fig. 5. Change of coil diameter with temperature after removing from DTA crucible

The DTA heating traces are presented on Fig. 3. For the cycles ranging from ambient temperature to 643K the curves (473K, 523K, 613K, 633K and 643K) are smooth

showing only glass transition at 617K. The two highest cycles (673K and 723K) contain the strong exothermic peak from crystallization with onset at 653K. The coils corresponding to the end of each DTA cycle are shown on Fig. 4. The coil heated to 473K has the largest external diameter (11,9 mm). This proves that the sample heated to 473K presents the largest reversible deformation. The diameters of the other samples are compared on Fig. 5. As it is seen, the second largest diameter (6,4 mm) has the sample heated to 523K, however at higher temperatures we can observe stabilization of the diameter at the average level of 5,7 mm. This shows that at the temperatures we observe stabilization of the deformation due to the viscous flow.

The X-ray diffraction pattern shows amorphous character of the melt-spun ribbon in as-cast state (Fig. 6, 293K). The patterns up to 643K have apparently no distinct peaks from crystalline phases (Fig. 6, 473K, 523K, 613K, 633K and 643K). However, the two highest cycles (673K and 723K) present the peaks from crystalline phases. They were identified as $(Ni,Cu,Fe)_3P$ phosphide and Ni(Cu,Fe) solid solution. Therefore the X-ray results seems to confirm the DTA observations because according to the expectations based on DTA traces, coils heated only to 673K and 723K should be crystalline.

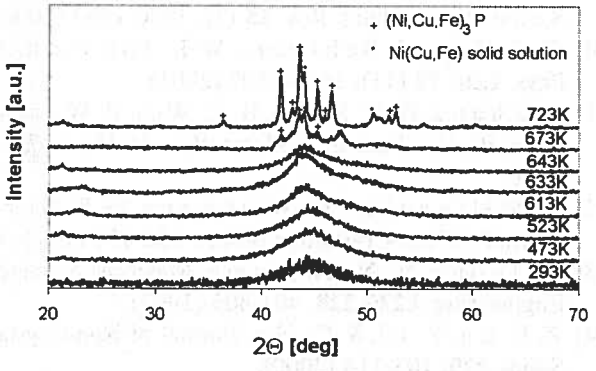

Fig. 6. X-ray patterns of the melt-spun $Ni_{63}Cu_9Fe_8P_{20}$ alloy registered after heating in DTA to different temperatures

The results of compression tests are shown on Fig. 7. As it is seen from the picture, up to the certain level, the increase of temperature influences the deformation process. The easiest deformation was observed in the test performed at 523K. Further increasing the temperature gradually elevated the force required for a given deformation. For example, Fig. 8 presents character of changes observed during the tests. The compressed samples soften above 473K with minimum force observed at 523K, and further increase of temperature leads to a gradual hardening. The attempts of deformation performed at higher temperatures (e.g. 673K) lead to crushing the samples (see Fig. 9).

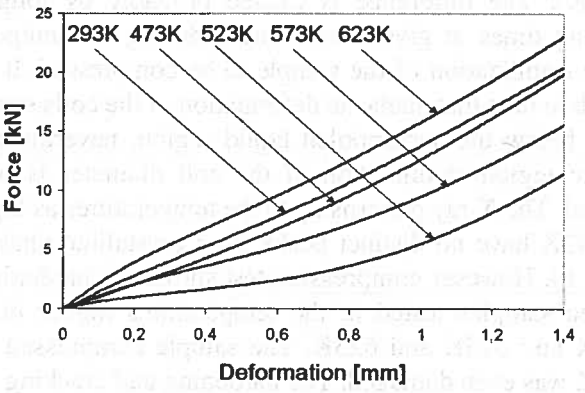

Fig. 7. The force-deformation characteristics for compression tests performed at different temperatures

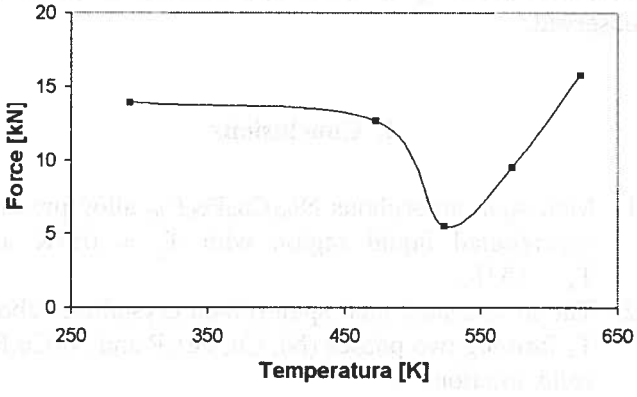

Fig. 8. The relation between force required for deformation by 1 mm at different test temperatures

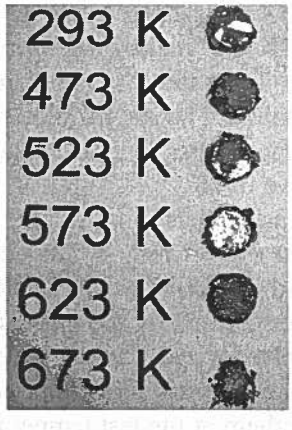

Fig. 9. The appearance of the samples compressed at different temperatures (brittleness of the sample compressed at 673K)

The observation of coil diameter and mechanical compression tests correlate well because both present possibility of viscous flow at elevated temperatures. However, the comparison of the DTA curves and results of compression tests shows that the supercooled region observed during heating at the rate of 10K/min is located at higher temperatures T_g = 617K and T_x = 653K than the easiest deformation during the compression test

(523K). The difference is caused probably by longer heating times at given temperature during the temperature stabilization of the sample to be compressed. It is worth to note that anelastic deformation of the coils starts even below the supercooled liquid region, nevertheless at the region stabilization of the coil diameter is observed. The X-ray patterns up to the temperatures as high as 643K have no distinct peaks from crystalline phases (Fig. 6). However compression test shows the hardening of the samples tested at the temperatures higher than 523K i.e.: 573K and 623K. The sample compressed at 673K was even damaged. The hardening and cracking of the samples may suggest crystallization of the samples. It is worth to note that, in the case of the heating interrupted after the crystallization peak i.e. for two coils heated in DTA up to 673K and 723K brittleness was observed.

4. Conclusions

1. Melt spun amorphous $Ni_{63}Cu_9Fe_8P_{20}$ alloy presents supercooled liquid region with T_g = 617K and T_x = 653K.
2. The investigated melt spun ribbon crystallizes above T_x forming two phases $(Ni, Cu, Fe)_3P$ and Ni(Cu,Fe) solid solution.
3. The ribbons coiled in a crucible and heated up to different temperatures show different amount of anelastic deformation. The largest deformation is observed between 473K and 523K. At higher temperatures i.e. 613K – 723K the unelastic deformation remains at the same level and the external diameter of the coils tends to stabilize. The stabilization may be explained by trespassing the supercooled liquid region that is located above 617K.
4. The compression tests show that the easiest deformation is observed between 473K and 573K with the smallest load occurring at 523K. At the test temperatures higher than 523K the increase of load can be observed. The increase could be explained by the crystallization process hardening the samples during holding them at the test temperatures sufficiently high to crystallize. The attempts of deformation performed at the 673K lead to crushing of the samples.

Received: 9 July 2005.

Acknowledgements

The financial support by the KBN research project No 4 T08D 005 24 is gratefully acknowledged.

REFERENCES

[1] A. Inoue, T. Nakamura, N. Nishiyama, T. Masumoto, Mater. Trans. JIM **33**, 937 (1990).
[2] A. Peker, W. L. Johnson, Appl. Phys. Lett. **63**, 2342 (1993).
[3] Y. He, R. B. Schwarz, J. I. Archuleta, Appl. Phys. Lett. **69**, 1861 (1996).
[4] K. Russew, B. J. Zappel, F. Sommer, Scripta Metallurgica et Materialia **32**, 271-276 (1995).
[5] Q. Wang, J. J. Blandin, M. Suery, J. M. Pelletier, Mat. Res. Soc. Symp. Proc. **754**, 315 (2003).
[6] Y. Kawamura, T. Shibata, A. Inoue, T. Masumoto, Acta Mater. **46**, 253-263 (1998).
[7] S. N. Nathaudhu, J. T. Im, R. E. Barber, I. E. Anderson, I. Karaman, K. T. Hartwig, Mat. Res. Soc. Symp. Proc. **754**, 191 (2003).
[8] Z. P. Lu, T. T. Goh, Y. Li, S. C. Ng, Acta Mater. **47** (7), 2215-2224 (1999).
[9] G. J. Fan, W. Loeser, S. Roth, J. Eckert, L. Schultz, J. Mater. Res. **15** (7), 1556-1563 (2000).
[10] C. C. Hays, J. Schroers, W. L. Johnson, Appl. Phys. Lett. **79** (11), 1605-1607 (2001).
[11] Y. Zhang, D. Q. Zhao, B. C. Wei, P. Wen, M. X. Pan, W. H. Wang, J. Mater. Res. **16** (6), 1675-1679 2001.
[12] R. Willnecker, K. Wittmann, G. P. Görler, Journal of Non-Crystalline Solids, 156-158 (1993) 450.
[13] A. Inoue, N. Nishiyama, Materials Science and Engineering **A226-228**, 401-405 (1997).
[14] Z. P. Lu, Y. Li, S. C. Ng, Journal of Non-Crystalline Solids **270**, 103-114 (2000).
[15] P. Villars, A. Prince, H. Okamoto, Handbook of Ternary Alloy Phase Diagrams, vols. 8 & 10, ASM International, The Materials Information Siciety, 1995.
[16] K. Ziewiec, P. Olszewski, R. Gajerski, S. Kąc, A. Ziewiec, Z. Kędzierski, Journal of Non-Crystalline Solids **343**, 150-153 (2004).